

# Journal Pre-proof

Highly efficient catalytic transfer hydrogenation of biomass-derived furfural to furfuryl alcohol using UiO-66 without metal catalysts

Mo Qiu, Tianmeng Guo, Ran Xi, Danni Li, Xinhua Qi



PII: S0926-860X(20)30312-4  
DOI: <https://doi.org/10.1016/j.apcata.2020.117719>  
Reference: APCATA 117719

To appear in: *Applied Catalysis A, General*

Received Date: 16 March 2020  
Revised Date: 19 June 2020  
Accepted Date: 22 June 2020

Please cite this article as: Qiu M, Guo T, Xi R, Li D, Qi X, Highly efficient catalytic transfer hydrogenation of biomass-derived furfural to furfuryl alcohol using UiO-66 without metal catalysts, *Applied Catalysis A, General* (2020), doi: <https://doi.org/10.1016/j.apcata.2020.117719>

This is a PDF file of an article that has undergone enhancements after acceptance, such as the addition of a cover page and metadata, and formatting for readability, but it is not yet the definitive version of record. This version will undergo additional copyediting, typesetting and review before it is published in its final form, but we are providing this version to give early visibility of the article. Please note that, during the production process, errors may be discovered which could affect the content, and all legal disclaimers that apply to the journal pertain.

© 2020 Published by Elsevier.

# Highly efficient catalytic transfer hydrogenation of biomass-derived furfural to furfuryl alcohol using UiO-66 without metal catalysts

Mo Qiu,<sup>[a], [d]</sup> Tianmeng Guo,<sup>[a]</sup> Ran Xi,<sup>[b]</sup> Danni Li,<sup>[b]</sup> Xinhua Qi,<sup>[b, c], \*</sup>

<sup>[a]</sup> *Agro-Environmental Protection Institute, Chinese Academy of Agricultural Sciences, No. 31, Fukang Road, Nankai District, Tianjin 300191, China*

<sup>[b]</sup> *College of Environmental Science and Engineering, Nankai University, No. 38, Tongyan Road, Jinnan District, Tianjin 300350, China*

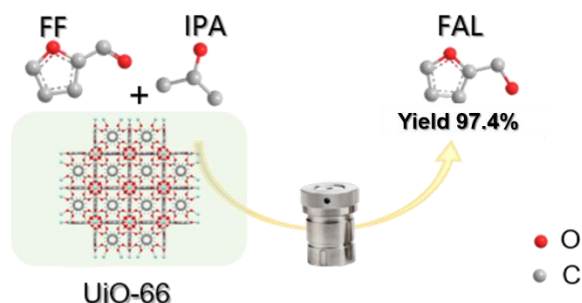
<sup>[c]</sup> *National & Local Joint Engineering Research Center of Biomass Resource Utilization, Tianjin 300350, China*

<sup>[d]</sup> *Key Laboratory of Advanced Energy Materials Chemistry (Ministry of Education), College of Chemistry, Nankai University, Tianjin 300071, China*

---

\* Corresponding author. Email: [qxinhua@nankai.edu.cn](mailto:qxinhua@nankai.edu.cn) (X. Qi); Tel (Fax): +86-22-2361-6651.

## Graphical abstract



This paper provides a promising strategy for the high yield production of FAL from the CTH of FF with UiO-66.

## Highlights

- 97% of FAL yield was obtained from the CTH of FF on UiO-66 in the IPA system.
- Lewis-acid and structural properties of MOFs are essential to the high yield of FAL.
- UiO-66 shows good recyclability and easy regeneration for producing FAL from FF.
- UiO-66 has a universal activity in the CTH of different aldehydes to alcohols in IPA.
- This CTH system open a promising route for yielding FAL from FF in large-scale.

## Abstract

In this paper, the as-prepared metal-organic frameworks material UiO-66 and other Zr-MOFs were directly used as catalytic transfer hydrogenation (CTH) catalysts to catalyze furfural (FF) to furfuryl alcohol (FAL) with 2-propanol (IPA) acted as both solvent and hydrogen donor. The results showed that the as-prepared UiO-66 had satisfactory catalytic activity and selectivity in

yielding FAL (97%) from the CTH of FF at 140 °C within 5 h. Moreover, the as-prepared UiO-66 exhibited relatively stable catalytic activity over five cycles and easy regeneration. Interestingly, UiO-66 was also applicable for the CTH of the other aldehydes such as 5-hydroxymethylfurfural, 5-methylfurfural, 4-methoxybenzaldehyde, and n-hexanal to the corresponding alcohols, affording high product yields up to 98%. This work provides a green, simple and sustainable process for the catalytic production of FAL from biomass-based furfural, which has certain significance for the sustainable utilization of biomass.

**Key words:** Biomass; catalytic transfer hydrogenation; furfural; furfuryl alcohol; Metal organic frameworks (MOFs).

## Introduction

The large-scale utilization of traditional fossil energy sources has caused energy crisis and environmental problems. Therefore, it is essential to fundamentally change the original energy use structure and find clean renewable energy which can replace fossil fuels. Among a number of renewable energy sources, biomass resources have attracted much attention due to their low pollution, wide distribution, environmental friendliness and abundant reserves [1, 2]. Nowadays, enormous effects have been made to convert lignocellulose biomass into high value-added products [3, 4].

Furfural (FF), as a most promising biomass-based platform chemical, which is dehydrated from biomass-based pentose, can be further converted into other useful chemicals such as furfuryl alcohol (FAL), furan, methyl furan, tetrahydrofuran (THF), tetrahydrofurfuryl alcohol

(THFAL), cyclopentone and olefins [5-8]. Among them, FAL is an important chemical intermediate, which is widely used in the production of synthetic fibers, lysine, thermosetting resins and vitamin C [9-12]. Therefore, the efficient production of FAL from FF is an important process in chemical industry. Since FF has a structural feature of the C=C bond in the furan ring and C=O in the branched chain, the efficient production of FAL requires selective hydrogenation of C=O bond rather than C=C bond [13]. Copper chromite is often used in industry as an efficient catalyst for this reaction, but it has the drawbacks of high toxicity, environment unfriendly and energy-intensive [14]. To develop more environmentally acceptable catalysts, a variety of gas and liquid-phase hydrogenation catalysts for the preparation of FAL from FF have been extensively developed [8, 15-18], including noble metals (Pd[15], Rh[16], Ru[19], and Pt[20]) and non-noble metals (Ni[17], Cu[21], and Co[22]). However, the harsh reaction conditions (high temperature and pressure) and the storage and transportation of external H<sub>2</sub> source have prompted researchers to develop alternative conversion methods.

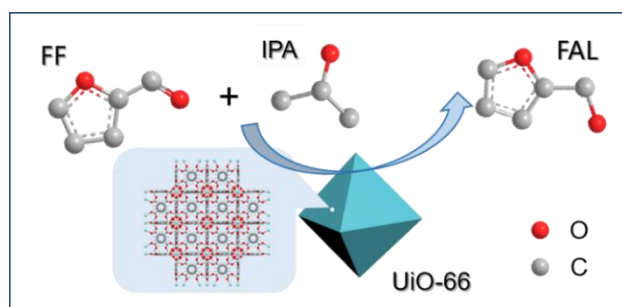
The catalytic transfer hydrogenation (CTH) is a hydrogenation reduction method for transferring hydrogen from hydrogen donor to target substrates without introducing external H<sub>2</sub> in the reaction process [23, 24]. Due to the process of CTH is high atomic economy, low energy consumption, non-toxicity, and high stability, it has been widely investigated in various hydrogenation reactions in recent years. Therefore, it is an intense demand to develop an eco-friendly, efficient, and sustainable catalyst for preparation of FAL from FF using CTH [25-27].

Metal-organic frameworks (MOFs) are a new type of porous organic-inorganic hybrid materials that have emerged in the past 20 years. MOFs have the advantages of large specific

surface area, adjustable pores and rich active centers, which enable the reactant molecules to diffuse inside of the MOFs effectively. Hence MOFs are often used as carriers or active centers in catalysis [28, 29], but they need to load other active centers, which makes their preparation process cumbersome and complicated. Some works also used MOFs as precursors to prepare novel catalysts. For example, Mondal et al. applied MOFs such as ZIF-67 and MIL-88B to synthesize novel metal oxide/C composites by in-situ pyrolysis, and the prepared MOF-based metal oxide/C composites showed excellent activity for the catalytic hydrogenation of biomass-derived furfural to tetrahydrofurfuryl alcohol (THFAL) and 2-methyl furan [30, 31]. UiO-66 is a kind of 3DMOFs materials which is composed of  $Zr_6O_4(OH)_4$  clusters and with outstanding hydrothermal stability [32-34]. Owing to the higher coordination number of Zr in the framework, UiO-66 has a Lewis acidity and exhibits excellent activity in the catalytic reaction [35, 36]. Moreover, according to the MPV (Meerwein-Ponndorf-Verley) reaction, aldehydes or ketones can be reduced by secondary alcohols under the action of Lewis acid catalyst, especially zirconium-based catalysts [37]. Consequently, it is possible for UiO-66 as a catalyst to catalyze FF to FAL.

Compared with the other MOFs-derived catalysts that need tedious post-functionalization step, in the present work, the as-prepared UiO-66 could be directly used as a CTH catalyst to catalyze FF to FAL (as shown in Scheme. 1). In this reaction system, IPA acted as both solvent and hydrogen donor to avoid using external  $H_2$ . Furthermore, the as-prepared UiO-66 was characterized and a series of hydrogenation experiments were carried out to investigate the activity of Zr-MOFs catalysts, the role of hydrogen donor and solvent, other aldehyde substrates and the recycling utilization of catalysts. The as-prepared UiO-66 was proved to have

satisfactory catalytic activity and selectivity in producing FAL from the hydrogenation of FF in the proposed system.



**Scheme 1** Scheme of the high yielding FAL from the CTH of FF with UiO-66 as catalyst in IPA solution.

## Experimental section

### Materials

The  $ZrCl_4$  (99%), 1, 4-dicarboxybenzene ( $H_2bdc$ ) (98%),  $H_2bdc-NH_2$  (98%), and 1,3,5-Benzenetricarboxylic acid ( $H_3btc$ ) (98%) were purchased from Sigma-Aldrich. Furfural (98%), furfural alcohol (98%), Methanol (99.8%), ethanol (98%), formic acid (99%), 1-propanol (99.5%), 2-propanol (99.5%), 2-butanol ( $\geq 99.5\%$ ), N,N-dimethylformamide(98%), acetic acid (99%), 5-hydroxymethylfurfural (98%), 2,5-furandimethanol (98%), 5-methylfurfural (99%), 5-methylfuran-2-methanol ( $\geq 95\%$ ), hexanal ( $\geq 95\%$ ), hexanol ( $\geq 95\%$ ), 4-methoxybenzaldehyde (98%), 4-methoxybenzyl alcohol (98%), cinnamaldehyde (98%) and cinnamic alcohol (98%) were obtained from Aladdin Agent Company.  $ZrO_2$  (<100 nm particle size) was purchased from Shanghai Macklin Biochemical Co., Ltd. (Shanghai, China). All chemicals were used as received without further purification.

### Synthesis of UiO-66(Zr)

Typically, 3.46 g (15 mmol) of  $ZrCl_4$  and 2.49 g (15 mmol) of  $H_2bdc$  were added to 150 mL

of DMF, then the mixture was stirred to get a clear solution. Subsequently, 1 mL ultrapure water and 25 mL acetic acid were sequentially added to the mixed solution while stirring. The resulting mixed solution was then transferred to a sealed 250 mL glass vial and placed in an oven at 120 °C for 24 h, after which it was cooled to ambient temperature. The synthesized UiO-66 was obtained via centrifugation, and washed 2-3 times with a mixed solution of methanol and DMF (v/v=1:4). The product was dried at 150 °C overnight in a vacuum oven for next use.

For comparisons, the other Zr-based MOFs including UiO-66-NH<sub>2</sub>, MOF-808 and MIL-140A were also synthesized by the solvothermal method according to the published papers [29, 33, 38, 39].

### **Characterization**

The as-prepared UiO-66, and the reused catalyst were characterized by different characterization techniques, including powder X-ray diffraction (XRD; Japan Rigaku, Cu-K $\alpha$ ), Fourier-transformed infrared spectroscopy (FT-IR; TENSOR 37, Germany), scanning electron microscopy (SEM; Gemini Sigma 300), thermogravimetric analysis (TGA; Shimadzu TA-60WS, in N<sub>2</sub> at a heating rate of 10 °C min<sup>-1</sup> up to 1000 °C), and N<sub>2</sub> adsorption-desorption isotherm curve (Micromeritics ASAP 2020, multipoint Brunauer–Emmett–Teller (BET) model and Horvath-Kawazoe (HK) pore size distribution calculation model). Bronsted and Lewis acid densities were determined by pyridine adsorption infrared (Py-IR) using a Nicolet 380 apparatus. The samples were pressed into thin wafers and evacuated in situ under vacuum at 250 °C for 2 h, and then cooled to 25 °C. Pyridine was dosed into the cell for 30 s. Subsequently, the system was evacuated at 150 °C and Py-IR spectra were recorded.

## Catalytic reaction and products analysis

In a standard procedure, a certain amount of FF (2, 3, 4 and 5 mmol) was dissolved in 10 mL of 2-propanol, then the solution was transferred into a 30 mL Teflon-lined stainless steel autoclave with addition of a certain amount of as-prepared UiO-66 (25, 50, 75 and 100 mg). Subsequently, the sealed autoclave was heated to a given temperature and maintained for a certain time. After reaction, the autoclave was cooled down quickly in a cold water bath, and the mixture was centrifuged to separate UiO-66 from the liquid product. Finally, the supernatant was diluted 100 times with IPA for quantitative analysis, and the catalyst was collected for use in another cycle experiment after washing with methanol and DMF several times and drying at 150 °C for 12 h in a vacuum oven.

The concentrations of FF and FAL in the reaction mixture were determined with an external standard method by gas chromatograph (Shimadzu, GC-2010 plus) equipped with a hydrogen flame ion (FID) detector and a Rtx-1701 column (30 m × 0.25 mm × 0.25 μm). The carrier gas was N<sub>2</sub>, and the column temperature was 270 °C, the detector temperature was 300 °C. Each reaction was repeated three times, and the standard deviation of the repeatability of FF conversion and FAL yield was within 3%.

## Results and discussion

### Catalytic conversion of FF to FAL by different MOFs

First, the catalytic hydrogenation of FF to FAL by various Zr-based MOFs (UiO-66, UiO-66-NH<sub>2</sub>, MOF-808, MIL-140A) with different coordination modes were investigated. The XRD patterns of these Zr-based materials are shown in Fig. S1, which are consistent with the previous reports [29, 33, 38, 39]. In addition, SEM images, FT-IR spectra, TG curves, N<sub>2</sub> adsorption-

desorption isotherms, and pore size distribution curves of the as-prepared Zr-MOFs were shown in Fig. S2-S5, which are consistent with those reported in the literatures [29, 33, 38, 39]. As shown in Table 1, all of the Zr-based MOFs were active for the catalytic hydrogenation of FF to FAL, but UiO-66 exhibited the best catalytic performance with a high FAL yield of 97%, which should be ascribed to its Lewis acidity and structural properties. UiO-66 is a 12-connected structure (12-connected with H<sub>2</sub>bdc) and has a structure of tetrahedral and octahedral cages, which is a 3D pore structure, and has a Lewis acid amount of 221.5  $\mu\text{mol/g}$ . The structure of UiO-66-NH<sub>2</sub> is similar to UiO-66, but -NH<sub>2</sub> is an electron-donating group, the electron cloud density on the benzene ring of UiO-66-NH<sub>2</sub> is higher than that of UiO-66, resulting in the decrease in the activity of the Lewis acid site (184.3  $\mu\text{mol/g}$ ). MOF-808 is 6-connected with H<sub>3</sub>btc, however, since it is also a 3D structure, which has the largest surface area, highest Lewis acid content in these Zr-based materials, but the yield of FAL (89%) was lower than UiO-66. In order to further explore the reason, the GC raw data of UiO-66 and MOF-808 (Fig. S6) indicated that more by-products obtained with MOF-808 as catalyst. In comparison, although MIL-140A is a 7-connected structure, because it is a triangular channels structure as 1D pore structure, and have the lowest Lewis acid site (137.7  $\mu\text{mol/g}$ ) which exhibited the lowest activities among all of the Zr-based MOFs. For nano-ZrO<sub>2</sub>, which has not the lowest amount of Lewis acid, but due to its lowest specific surface area, it has the worst activity among the Zr-based materials. Therefore, combining the Py-IR results of these Zr-based materials (Fig. S7), the Lewis acidity and structural characteristics of the catalyst are the key for the catalytic conversion of FF to FAL. To further explore the relationship between material structure and activity, detailed characterization and investigation will be conducted for UiO-66.

**Table 1** CTH of FF to FAL over different Zr-MOFs and nano-ZrO<sub>2</sub>.

Entry	Catalysts	S <sub>BET</sub> (m <sup>2</sup> /g)	L-acid amount (μmol/g)	Conv. (%)	Y <sub>FAL</sub> (%)
1	UiO-66	966	221.5	>99	97
2	UiO-66-NH <sub>2</sub>	711	184.3	60	42
3	MOF-808	1301	245.2	>99	89
4	MIL-140A	291	137.7	27	12
5	nanoZrO <sub>2</sub>	14	164.4	13	6

Reaction conditions: 10 mL IPA used as solvent and hydrogen donor, 140 °C, 5 h, 75 mg of catalyst, and 3 mmol of substrate.

### Characterization of the as-prepared UiO-66

As shown in Fig. 1, the XRD diffraction pattern of UiO-66 synthesized in this work has good coincidence with that of the UiO-66 in the crystallographic data, and two diffraction peaks at  $2\theta = 7.4^\circ$  and  $8.5^\circ$  correspond to the (111) and (002) crystal planes, respectively. The peak at  $2\theta = 12^\circ$  corresponding to (220) crystal plane is caused by the guest molecules in the pores. XRD patterns show that UiO-66 was successfully synthesized with high crystallinity.

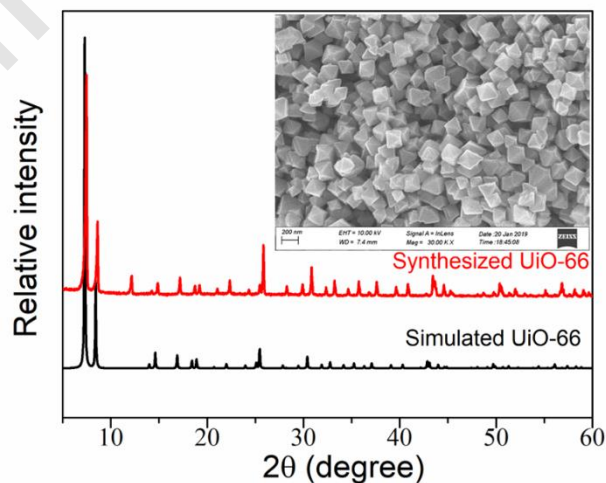


**Fig. 1** XRD patterns of the as-synthesized UiO-66 and the simulated UiO-66.

Fig. 2a shows the FT-IR spectrum of UiO-66. Peaks at  $1506\text{ cm}^{-1}$  and  $1590\text{ cm}^{-1}$  were caused by the stretching vibration of C=C in the benzene ring of the organic ligand H<sub>2</sub>bdc. The peak at  $1391\text{ cm}^{-1}$  corresponds to the stretching vibration of the -COOH. The in-plane bending vibration of C-H in the benzene ring causes diffraction peaks at  $1161\text{ cm}^{-1}$  and  $1095\text{ cm}^{-1}$ . The peaks at  $485\text{ cm}^{-1}$  and  $667\text{ cm}^{-1}$  are attributed to in-plane and out-of-plane bending vibrations of COO-. In particular, the peak appearing at  $550\text{ cm}^{-1}$  being the characteristic vibration of Zr-O further proves the existence of the UiO-66 structure [32].

To investigate the thermal stability of the synthesized UiO-66, TG analysis was performed in nitrogen atmosphere. As shown in Fig. 2b. The mass loss from room temperature to  $100\text{ }^{\circ}\text{C}$  was due to the evaporation of water adsorbed in the pores. The mass loss of about 15% in the range of  $100\text{ }^{\circ}\text{C}$  to  $300\text{ }^{\circ}\text{C}$  was caused by the evaporation of DMF in the channel and the dehydroxylation process. During this process, the hydroxyl groups bound to the center of the metal ion was detached in the form of water molecules, thereby changing the coordination environment of Zr center, and the Lewis acidity was also obtained. The Lewis acidity of UiO-66 could be maintained below  $300\text{ }^{\circ}\text{C}$ , thus, the catalyst has Lewis acid under our experimental conditions. When the temperature was higher than  $500\text{ }^{\circ}\text{C}$ , the organic ligand H<sub>2</sub>bdc gradually decomposed, proving that UiO-66 had superior thermal stability and could maintain structural integrity below  $500\text{ }^{\circ}\text{C}$ . At about  $600\text{ }^{\circ}\text{C}$ , the skeleton structure of UiO-66 was completely decomposed, and remained ZrO<sub>2</sub>@C.

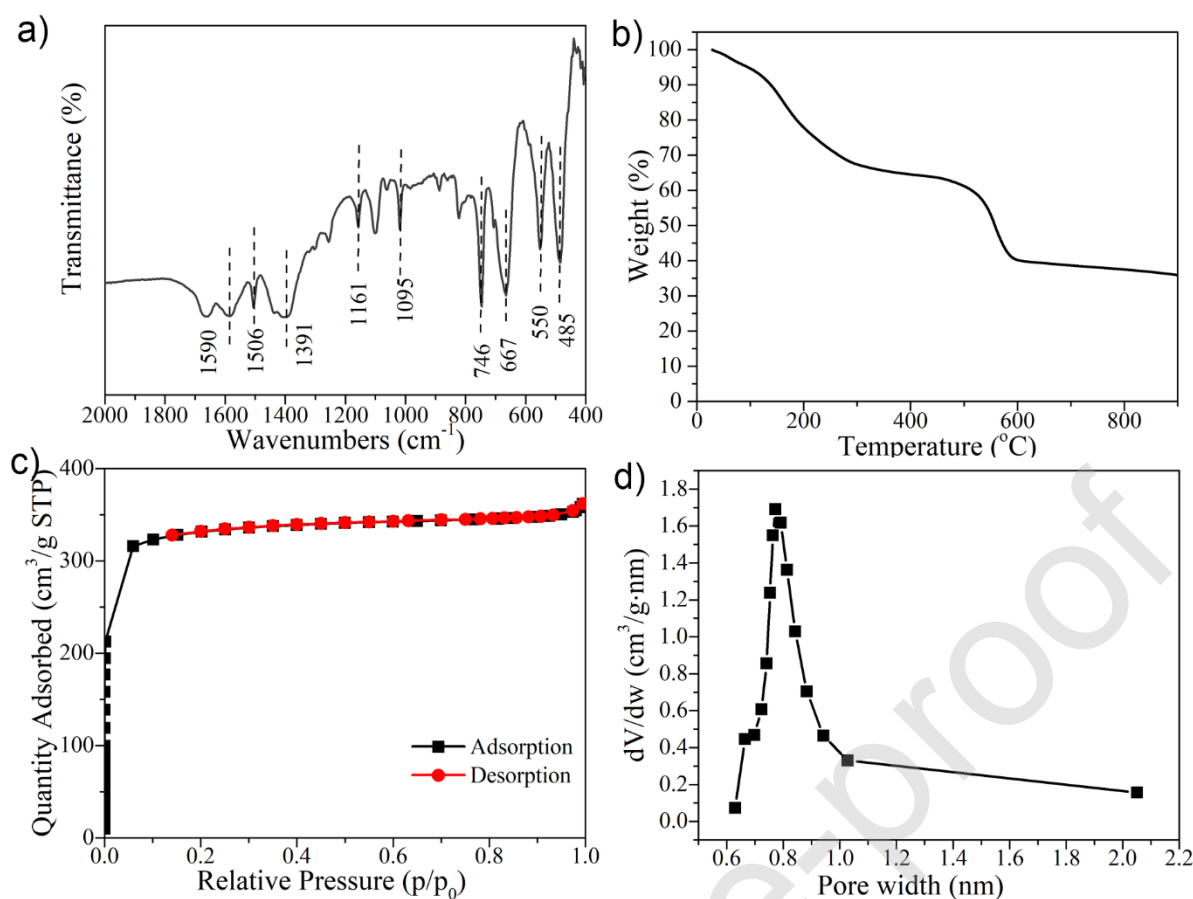


**Fig. 2** a) FT-IR spectrum, b) TG curve, c) N<sub>2</sub> adsorption-desorption isotherm and d) pore size distribution curve of the as-prepared UiO-66.

The N<sub>2</sub> adsorption-desorption isotherm curve of the sample is shown in Fig. 2c, which shows a typical type I isotherm, indicating that the synthesized UiO-66 is a typical microporous material. Fig. 2d shows the pore size distribution of UiO-66 obtained by the HK model. UiO-66 has a large BET specific surface area of 966 m<sup>2</sup>/g, a total pore volume of 0.56 cm<sup>3</sup>/g, and an average pore diameter of 0.77 nm.

### CTH activity of UiO-66 for conversion of FF to FAL

The effect of the amount of FF on the reaction efficiency was investigated. A certain amount (2, 3, 4, and 5 mmol) of FF was added to 10 mL IPA, then the FF conversion and the FAL yield were determined after reaction at 140 °C for 3 h. As can be seen from Fig. 3, FF could be

converted completely in the range of 2–4 mmol initial addition amount. When the adding amount of FF was increased to 5 mmol, the conversion decreased slightly. The yield of FAL reached the maximum value of 98% when the amount of FF was 3 mmol, indicating that the amount of catalyst was sufficient to completely convert FF under this reaction condition. Therefore, in the subsequent testing process, the amount of FF was chose to be 3 mmol.

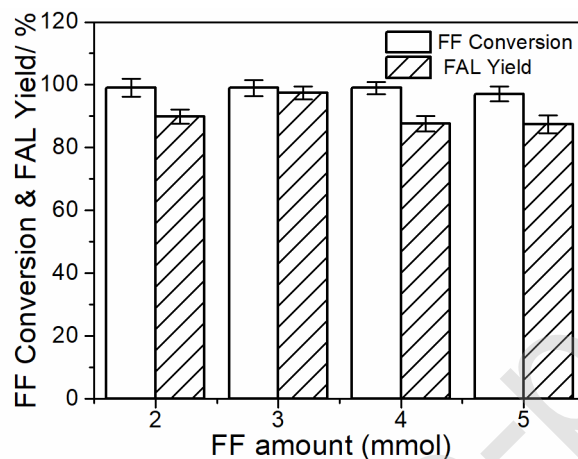


**Fig. 3** Influence of the initial amounts of FF on the FAL yield catalyzed by UiO-66 (75 mg UiO-66, 10 mL IPA, 140 °C, 5 h).

The effect of the amount of UiO-66 on the catalytic was examined in the range of 25–100 mg (140 °C, 3 h). The results are shown in Fig. 4. When 25 mg UiO-66 was used, the conversion of FF reached only 80% with a FAL yield of 68%. When the addition amount of the catalyst was increased to more than 50 mg, the FF was converted completely. The yield of FAL increased as the amount of catalyst increased, and the highest FAL yield 98% was achieved at a catalyst loading amount of 75 mg. The further increase in UiO-66 addition amount did not affect the conversion and yield.

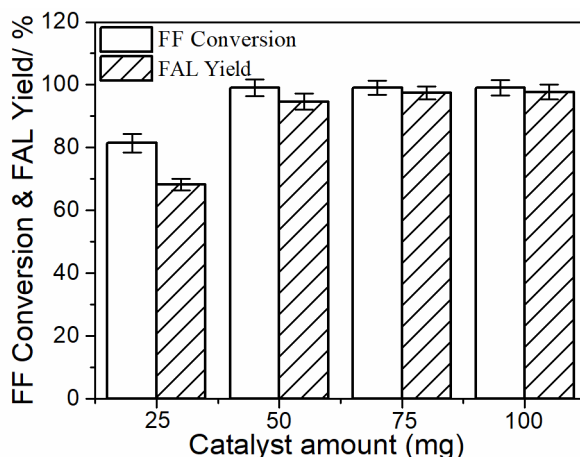


**Fig. 4** Influence of the UiO-66 amounts on the FAL yield (3 mmol FF, 10 mL IPA, 140 °C, 5 h).

The effect of reaction temperature and time on the catalytic hydrogenation of FF to FAL were explored and the results are shown in Fig. 5. It can be seen from Fig. 5a that the temperature had a great influence on the conversion of FF. When the reaction temperature was 120 °C, the conversion of FF was only 70% with a FAL yield of 54% even if the reaction time was as long as 7 h. When the temperature was raised to 140 °C, the FF could be almost completely converted in 5 h (>99%) with a FAL yield of 97%. The temperature continued to rise and the time required for complete conversion of FF was further shortened, however, the yield of FAL first increased and then decreased slightly, since the CTH of FF to FAL is one step in a series of cascade reaction, and excessive hydrogenation could be occurred to form the other by-products such as furan, methyl furan, tetrahydrofuran (THF), tetrahydrofurfuryl alcohol (THFAL) [5-8], and FAL itself would also undergo polymerization reaction. The yield of FAL (Fig. 5b) maintained at a high level of more than 80% in the range of 140-180 °C, with the highest selectivity of 97% at 140 °C for 5 h, indicating that FF could be hydrogenated with high selectivity to produce FAL by the as-prepared UiO-66. In this reaction condition, the yield of FAL with MOF-808 as the catalyst, is lower than UiO-66 because of more by-products produced (Fig. S7). Therefore,

the effect of reaction temperature and time on the catalytic hydrogenation of FF to FAL with MOF-808 were explored and the results are shown in Fig. S8. Compared with UiO-66, MOF-808 at the same reaction temperature and reaction time, it is easy to excessively hydrogenate to produce by-products, but it has certain advantages at low temperatures. Moreover, scaled-up CTH reaction was also carried out to further investigate the activity of UiO-66. The reaction was conducted with 20 mmol FF loading in the presence of 75 mg UiO-66 in 25 mL IPA at 170 °C for 10 h, and a FAL yield of 71% could be achieved. Therefore, UiO-66 has the potential in industrial production of FAL by the CTH reaction of FF.

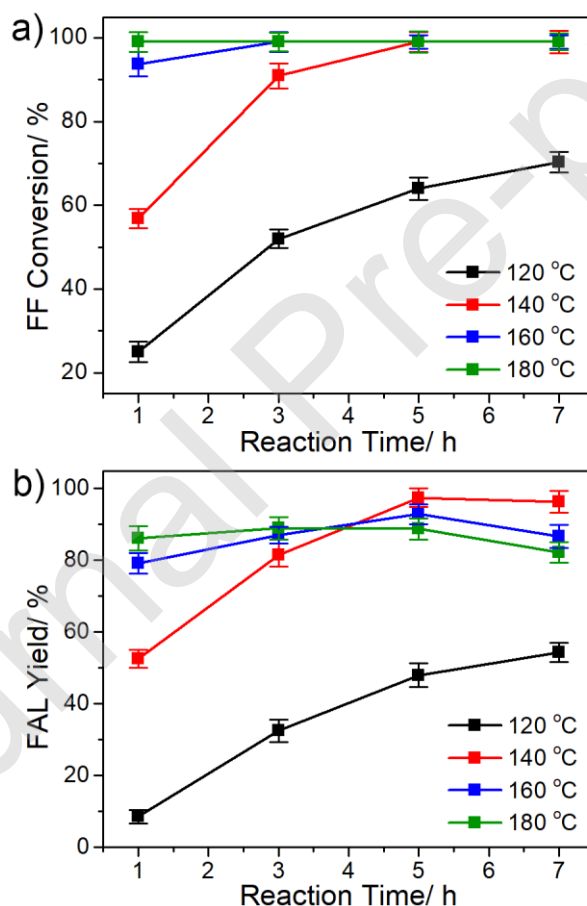


**Fig. 5** Influence of reaction temperature and time on a) the FF conversion and b) FAL Yield (3 mmol FF, 75 mg UiO-66, 10 mL IPA).

The kinetics of the CTH reaction of FF to FAL catalyzed by UiO-66 was also studied. As

shown in Fig. 6, in a short reaction time (30–120 min), when the reaction temperature was increased from 120 to 160 °C, the first-order reaction rate constant  $k$  rose from 0.00686 to 0.02163 min<sup>-1</sup>. According to the Arrhenius equation, the activation energy of the system was calculated to be 40.5 kJ/mol. Table 2 lists the activity data and activation energy of other catalysts reported in the published papers for the FF to FAL reaction. As shown in Table 2, compared with other catalysts used in the CTH reaction of FF to FAL, the UiO-66 catalyst has great advantages.

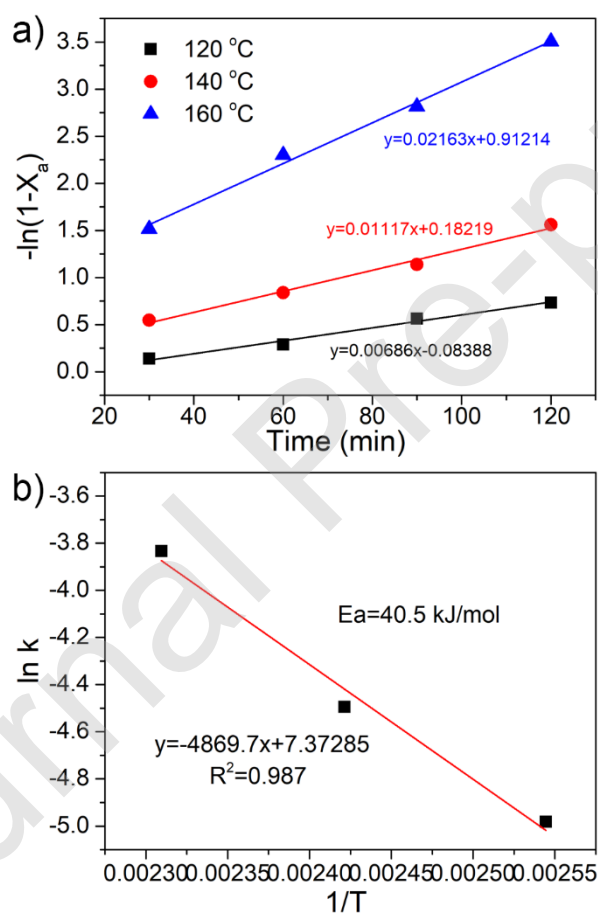


**Fig. 6** (a) Kinetic study of the FF to FAL conversion by UiO-66 as catalyst ( $X_a$  is the conversion of FF) and (b) Arrhenius plot of conversion of FF over UiO-66 (3 mmol FF, 75 mg UiO-66, 10 mL IPA).

**Table 2** Comparison of the catalysis activity of the as-prepared UiO-66 and other reported

catalyst toward the CTH of FF to FAL using IPA as H-donor.

Catalyst	FAL (mmol)	Cat. (mg)	Temp. (°C)	Time (h)	IPA (mL)	Conv. (%)	Yield (%)	E <sub>a</sub> (kJ/mol)	Ref.
BZC	0.67	100	30	24	20	97.7	96.7	53.6	[40]
Pd/Fe <sub>2</sub> O <sub>3</sub>	0.4	500	150	7.5	40	66.0	37.0	46.8	[41]
γ-Fe <sub>2</sub> O <sub>3</sub> @HAP	1	40	180	10	15	96.2	91.7	47.7	[24]
ZrPN	2.5	100	140	2	10	98.0	98.0	70.5	[42]
Al-Zr@Fe	2	40	180	4	10	99.1	90.4	45.3	[23]
DUT-69	1	100	120	4	5	95.9	92.2	29.5	[43]
Nano-NiO	2	80	150	4	10	84.6	80.9	45.1	[25]
UiO-66	3	75	140	5	10	>99	97	40.5	This work
UiO-66	3	75	180	1	10	>99	87	40.5	This work

The recycling performance of the UiO-66 catalyst was investigated under the optimal conditions for the production of FAL from FF. As shown in Fig. 7, in the first use, the conversion of FF exceeded 99% and the yield of FAL was 97% after 5 h at 140 °C. After the catalyst was recovered, it was directly used in the second reaction without any treatment, and the conversion of FF still exceeded 99% and the yield of FAL was 93% at 140 °C in 5 h reaction time. A FAL yield of 88% was obtained when the catalyst was used for the third time. At the fifth cycle, the conversion of FF was 97%, and the yield of FAL decreased to 80%, indicating that the activity of the catalyst had slightly decreased. However, the conversion of FF can be restored to 99% and a FAL yield of 95% could be regained after the regeneration of catalyst UiO-66 by calcining at 300 °C for 2 h, demonstrating that UiO-66 had excellent reactivity and cycle recyclability. To find the reason of the decrease in activity of the catalysts without regeneration, we performed a series of characterizations to the used catalyst for five times.

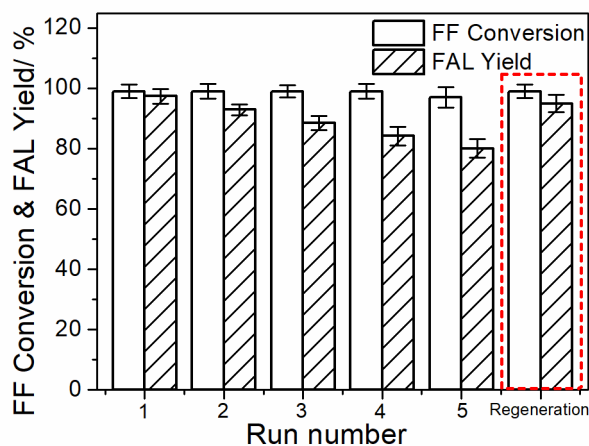


**Fig. 7** Recycle performance of UiO-66 on FF to FAL (3 mmol FF, 75 mg UiO-66, 10 mL IPA, 140 °C, 5h).

The color of the catalyst changed from the original white to yellow after the reaction was completed. The catalyst was washed with methanol and DMF under ultrasonic conditions, but it still could not return to the original white color. Then, the XRD patterns and FT-IR spectra of UiO-66 before and after the reaction were compared in Fig. 8. After the reaction was carried out for five times, UiO-66 still maintained a complete crystal structure. The XRD peaks and FT-IR spectra did not change significantly, indicating that the UiO-66 stayed good stability under the reaction conditions and the decrease in catalyst activity was not caused by the collapse of UiO-66 framework. In addition, compared with the fresh UiO-66, the BET surface area of the catalyst after reused for five times was reduced to 703 m<sup>2</sup>/g. Hence, the possible deactivation reason is the deposition of generated polymers on the UiO-66.

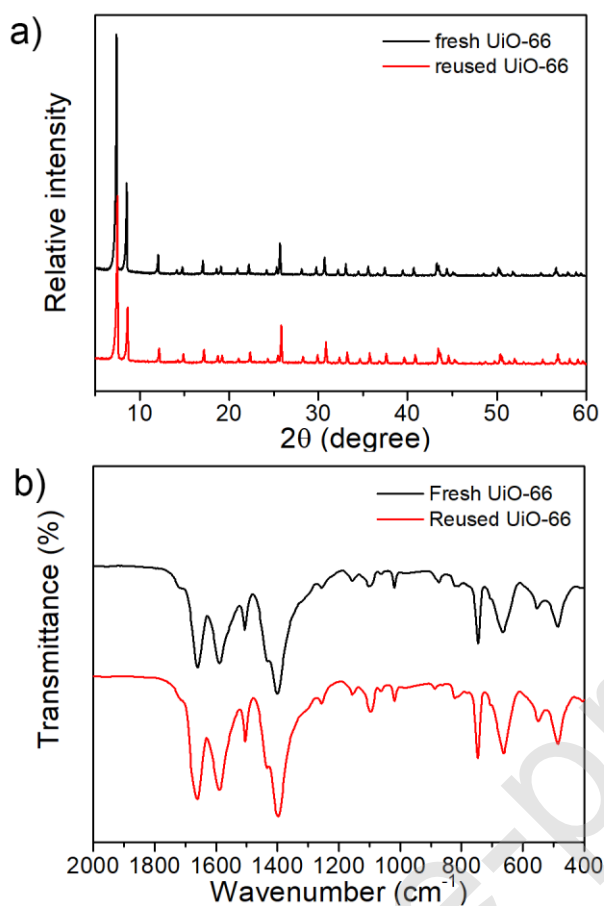
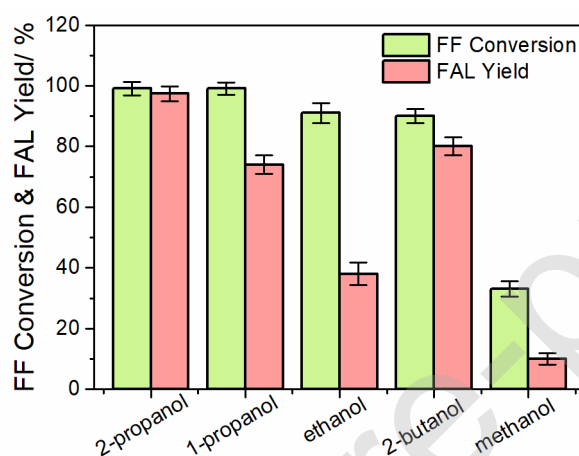


**Fig. 8** a) XRD patterns, and b) FT-IR spectra of the fresh UiO-66 and reused UiO-66 catalysts.

When FF reacted in IPA system, the hemiacetal reaction occurred between them to produce isopropoxydecyl alcohol. Besides, FF and the intermediate isopropoxydecyl alcohol would also polymerize under high reaction temperature, generating some oligomeric organic matter to deposit on the UiO-66 catalyst and block part of the catalytic active sites, thus preventing their sufficient contact with FF and leading to the slight decrease in FAL yield. After regeneration, the BET surface area of the catalyst was increased to 892 m<sup>2</sup>/g, which might lead to the increase of hydrogenation activity (Figure 7).

Different hydrogen donors including methanol, ethanol, 2-butanol, 1-propanol and IPA used in the CTH reaction of FF to FAL catalyzed by UiO-66 were examined (Fig. 9). It shows that

all of the used alcohols were effective hydrogen donors for the hydrogenation of FF to FAL. Compared with primary alcohols (methanol, ethanol and 1-propanol), secondary alcohols (IPA) as a hydrogen donor could give higher FAL yield, which is generally due to the fact that secondary alcohols have lower reduction potential than primary alcohols [44]. For 2-butanol, its activity is slightly lower than that of IPA due to the steric effect caused by its longer carbon chain.

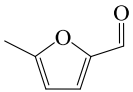
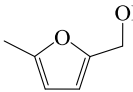
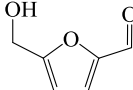
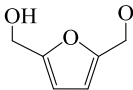
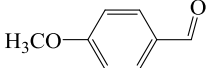
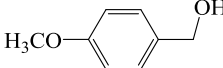
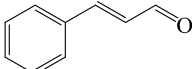
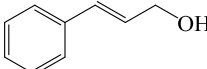
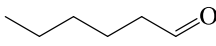
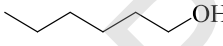


**Fig. 9** CTH of FF to FAL with UiO-66 using different H-donors (3 mmol FF, 75 mg UiO-66, 10 mL H-donors, 140 °C, 5h).

The activity and universality of UiO-66 for the selective catalytic conversion of the other aldehydes to the corresponding alcohols were investigated under the conditions of IPA as hydrogen donor (160–180 °C). As shown in Table 3, UiO-66 showed high activity in the CTH reaction of several aldehydes to alcohols. Relatively high reaction temperature was required for the catalytic hydrogenation of 5-hydroxymethylfurfural and 5-methylfurfural (Entry 1 and 2) resulted from the steric hindrance effect due to the presence of substituents [25]. UiO-66 exhibited high activity for benzene ring-containing aldehydes (4-methoxybenzaldehyde), with 92% yield and 98% selectivity. In addition, cinnamaldehyde as substrate could maintain selective hydrogenation for C = O bonds instead of C = C bonds (Entry 4), and UiO-66 showed

such a high activity for the catalytic hydrogenation of n-hexanal that a n-hexanol yield of 98% was achieved (Entry 5). Therefore, the UiO-66 has good universality for the CTH reaction of various aldehydes to alcohols.

**Table 3** CTH activity of UiO-66 for different aldehyde compounds.

Entry	Substrate	Product	Temp. (°C)	Time (h)	Conv. (%)	Yield (%)	Select. (%)
1			180	6	84	75	90
2			180	4	87	82	94
3			170	2	94	92	98
4			160	6	71	67	95
5			180	6	>99	98	99

Reaction conditions: 2 mmol substrate, 75 mg UiO-66, 10 mL IPA.

### Reaction mechanism for the catalytic hydrogenation of FF to FAL by UiO-66

The following steps are proposed for the mechanism of aldehyde to alcohol catalyzed by UiO-66 in IPA acting as both solvent and hydrogen donor. First, the alcohol was adsorbed on the Zr-O clusters of UiO-66 framework, and the basic site of COO<sup>-</sup> in the carboxyl group promoted the deprotonation of IPA. Subsequently, IPA was dissociated into the corresponding alkoxide ion and active hydrogen atoms under the double roles of the acid-base sites of Zr<sup>4+</sup>-O<sup>2-</sup>. In the process of catalytic conversion of FF by UiO-66, the carbonyl group of FF was also activated by Lewis acidic site of Zr<sup>4+</sup>. Then, hydrogen transfer occurred between the dissociated

alkoxide ion and the activated FF to produce acetone and FAL, which are dissociated and desorbed from UiO-66 rapidly so that the active site on UiO-66 can be regenerated. This process is consistent with the reported literatures [25, 27, 35].

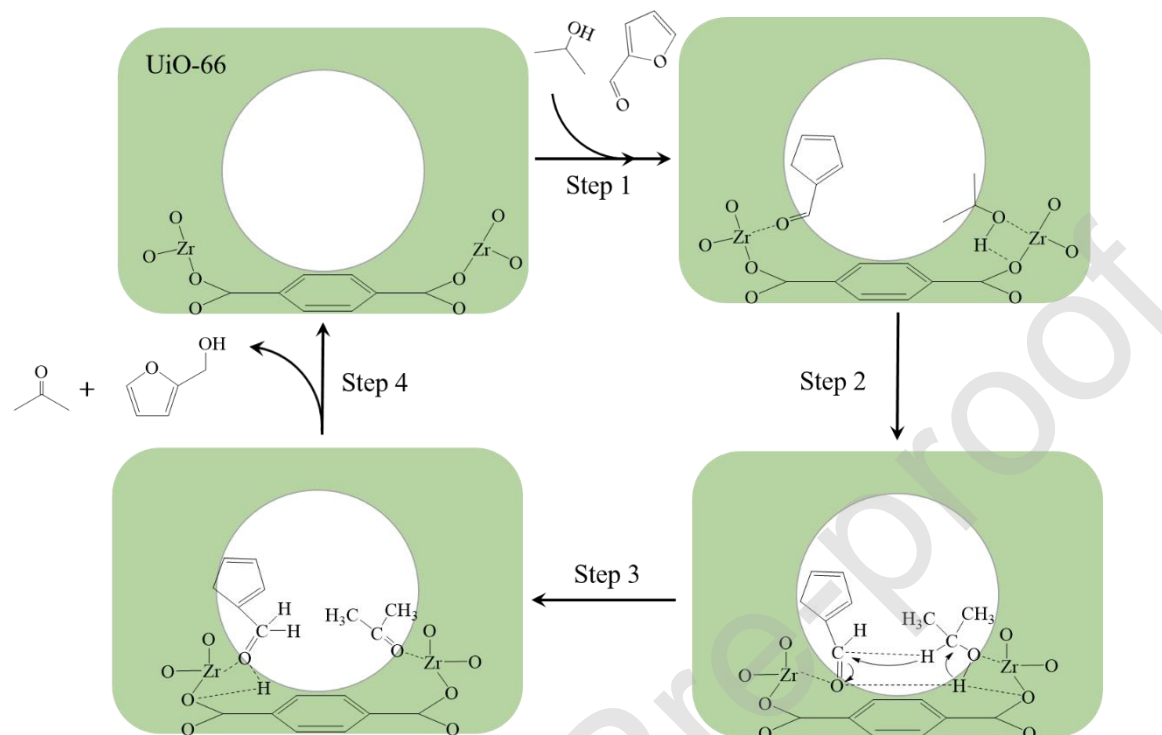


**Fig. 10** Possible CTH reaction mechanism for FF to FAL with UiO-66 as catalyst.

## Conclusion

In summary, several different Zr-based MOFs (UiO-66, UiO-66-NH<sub>2</sub>, MOF-808 and MIL-140A) were prepared for CTH of FF to FAL. Due to the different Lewis-acid properties caused by their own structural characteristics, UiO-66 exhibited the best catalytic performance of CTH of FF to FAL at high temperature. The conversion of FF exceeded 99% and the yield of FAL was 97% after 5 h at 140 °C in the IPA solution. Moreover, the as-prepared UiO-66 catalyst exhibited relatively stable catalytic activity over five cycles with FAL yields up to 80% remaining, and the yield of FAL can return to 95% after the regeneration of UiO-66 by calcination. Furthermore, a possible reaction mechanism was proposed, demonstrating that the

Lewis acidity of UiO-66 and its structural characteristics are the essential reasons for its high activity in the CTH of FF to FAL. Besides, UiO-66 also showed a universal catalytic activity in the CTH of different aldehydes to produce corresponding alcohols in the presence of IPA. This work provides an efficient and sustainable process for the high-yield production of FAL from the CTH of biomass-derived FF in IPA solutions, and offers wide application for the transformation of biomass based substrates into valuable chemicals.

#### CRedit authorship contribution statement

M. Q. and X.Q. conceived the concept and directed the project. M. Q., T. G., R. X. and D. L. conducted the experiments and analyses. M. Q. and X.Q. discussed the results and in charge of the preparation and revision of the manuscript.

#### Declaration of interests

The authors declare that they have no known competing financial interests or personal relationships that could have appeared to influence the work reported in this paper.

#### Acknowledgements

The authors greatly appreciate the financial support from the Natural Science Foundation of Tianjin (No.17JCQNJC05700), the National Natural Science Foundation of China (NSFC, nos. 21876091 and 21577073), and the Natural Science Fund for Distinguished Young Scholars of Tianjin (No. 17JCJQJC45500).

#### Supporting Information

Supplementary data associated with this article can be found in the online version.

**Reference**

- [1] E.J. Cho, L.T.P. Trinh, Y. Song, Y.G. Lee, H.-J. Bae, *Bioresour. Technol.*, 298 (2020) 122386.
- [2] L.T. Mika, E. Cséfalvay, Á. Németh, *Chem. Rev.*, 118 (2018) 505-613.
- [3] R. Kumar, V. Strezov, H. Weldekidan, J. He, S. Singh, T. Kan, B. Dastjerdi, *Renew. Sustain.Energ. Rev.*, 123 (2020) 109763.
- [4] S. Zhu, J. Xu, Z. Cheng, Y. Kuang, Q. Wu, B. Wang, W. Gao, J. Zeng, J. Li, K. Chen, *Appl. Catal. B-Environ.*, 268 (2020) 118732.
- [5] Y. Leng, L. Shi, S. Du, J. Jiang, P. Jiang, *Green Chem.*, 22 (2020) 180-186.
- [6] Y. Cao, H. Zhang, K. Liu, Q. Zhang, K.-J. Chen, *ACS Sustain. Chem. Eng.*, 7 (2019) 12858-12866.
- [7] H. Niu, J. Luo, C. Li, B. Wang, C. Liang, *Ind. Eng. Chem. Res.*, 58 (2019) 6298-6308.
- [8] Y. Nakagawa, M. Tamura, K. Tomishige, *ACS Catal.*, 3 (2013) 2655-2668.
- [9] Y.-C. He, C.-X. Jiang, J.-W. Jiang, J.-H. Di, F. Liu, Y. Ding, Q. Qing, C.-L. Ma, *Bioresour. Technol.*, 238 (2017) 698-705.
- [10] N. Guigo, A. Mija, L. Vincent, N. Sbirrazzuoli, *Phys. Chem. Chem. Phys.*, 9 (2007) 5359-5366.
- [11] B. Ren, C. Zhao, L. Yang, G. Fan, F. Li, *Appl. Surf. Sci.*, 504 (2020) 144364.
- [12] H. Deka, M. Misra, A. Mohanty, *Ind. Crop. Prod.*, 41 (2013) 94-101.
- [13] R. Mariscal, P. Maireles-Torres, M. Ojeda, I. Sádaba, M. López Granados, *Energ. Environ. Sci.*, 9 (2016) 1144-1189.

- [14] R. Rao, A. Dandekar, R.T.K. Baker, M.A. Vannice, *J. Catal.*, 171 (1997) 406-419.
- [15] J. Du, J. Zhang, Y. Sun, W. Jia, Z. Si, H. Gao, X. Tang, X. Zeng, T. Lei, S. Liu, L. Lin, *J. Catal.*, 368 (2018) 69-78.
- [16] F. Toledo, I.T. Ghampson, C. Sepúlveda, R. García, J.L.G. Fierro, A. Videla, R. Serpell, N. Escalona, *Fuel*, 242 (2019) 532-544.
- [17] J. Parikh, S. Srivastava, G.C. Jadeja, *Ind. Eng. Chem. Res.*, 58 (2019) 16138-16152.
- [18] C.P. Jiménez-Gómez, J.A. Cecilia, D. Durán-Martín, R. Moreno-Tost, J. Santamaría-González, J. Mérida-Robles, R. Mariscal, P. Maireles-Torres, *J. Catal.*, 336 (2016) 107-115.
- [19] P. Panagiotopoulou, D.G. Vlachos, *Appl. Catal. A-Gen.*, 480 (2014) 17-24.
- [20] M.J. Taylor, L.J. Durndell, M.A. Isaacs, C.M.A. Parlett, K. Wilson, A.F. Lee, G. Kyriakou, *Appl. Catal. B-Environ.*, 180 (2016) 580-585.
- [21] H. Du, X. Ma, P. Yan, M. Jiang, Z. Zhao, Z.C. Zhang, *Fuel Process. Technol.*, 193 (2019) 221-231.
- [22] Y. Wang, Y. Lu, Q. Cao, W. Fang, *Chem. Commun.*, 56 (2020) 3765-3768.
- [23] J. He, H. Li, A. Riisager, S. Yang, *ChemCatChem*, 10 (2018) 430-438.
- [24] F. Wang, Z. Zhang, *ACS Sustain. Chem. Eng.*, 5 (2017) 942-947.
- [25] J. He, L. Schill, S. Yang, A. Riisager, *ACS Sustain. Chem. Eng.*, 6 (2018) 17220-17229.
- [26] R. López-Asensio, J.A. Cecilia, C.P. Jiménez-Gómez, C. García-Sancho, R. Moreno-Tost, P. Maireles-Torres, *Appl. Catal. A-Gen.*, 556 (2018) 1-9.
- [27] C.K.P. Neeli, Y.-M. Chung, W.-S. Ahn, *ChemCatChem*, 9 (2017) 4570-4579.
- [28] Q. Yuan, D. Zhang, L.v. Haandel, F. Ye, T. Xue, E.J.M. Hensen, Y. Guan, *J. Mol. Catal. A-Chem.*, 406 (2015) 58-64.

- [29] J. Jiang, F. Gándara, Y.-B. Zhang, K. Na, O.M. Yaghi, W.G. Klemperer, *J. Am. Chem. Soc.*, 136 (2014) 12844-12847.
- [30] S. Pendem, S.R. Bolla, D.J. Morgan, D.B. Shinde, Z. Lai, L. Nakka, J. Mondal, *Dalton Trans.*, 48 (2019) 8791-8802.
- [31] P. Koley, S. Chandra Shit, B. Joseph, S. Pollastri, Y.M. Sabri, E.L.H. Mayes, L. Nakka, J. Tardio, J. Mondal, *ACS Appl. Mater. Interfaces*, 12 (2020) 21682-21700.
- [32] J.H. Cavka, S. Jakobsen, U. Olsbye, N. Guillou, C. Lamberti, S. Bordiga, K.P. Lillerud, *J. Am. Chem. Soc.*, 130 (2008) 13850-13851.
- [33] H. Furukawa, F. Gándara, Y.-B. Zhang, J. Jiang, W.L. Queen, M.R. Hudson, O.M. Yaghi, *J. Am. Chem. Soc.*, 136 (2014) 4369-4381.
- [34] H. Wu, Y.S. Chua, V. Krungleviciute, M. Tyagi, P. Chen, T. Yildirim, W. Zhou, *J. Am. Chem. Soc.*, 135 (2013) 10525-10532.
- [35] Y. Kuwahara, H. Kango, H. Yamashita, *ACS Sustain. Chem. Eng.*, 5 (2017) 1141-1152.
- [36] A.H. Valekar, K.-H. Cho, S.K. Chitale, D.-Y. Hong, G.-Y. Cha, U.H. Lee, D.W. Hwang, C. Serre, J.-S. Chang, Y.K. Hwang, *Green Chem.*, 18 (2016) 4542-4552.
- [37] F. Gonell, M. Boronat, A. Corma, *Catal. Sci. Technol.*, 7 (2017) 2865-2873.
- [38] L. Shen, W. Wu, R. Liang, R. Lin, L. Wu, *Nanoscale*, 5 (2013) 9374-9382.
- [39] V. Guillerm, F. Ragon, M. Dan-Hardi, T. Devic, M. Vishnuvarthan, B. Campo, A. Vimont, G. Clet, Q. Yang, G. Maurin, G. Férey, A. Vittadini, S. Gross, C. Serre, *Angew. Chem. Int. Ed.*, 51 (2012) 9267-9271.
- [40] M. Ma, P. Hou, J. Cao, H. Liu, X. Yan, X. Xu, H. Yue, G. Tian, S. Feng, *Green Chem.*, 21 (2019) 5969-5979.

- [41] D. Scholz, C. Aellig, I. Hermans, *ChemSusChem*, 7 (2014) 268-275.
- [42] H. Li, J. He, A. Riisager, S. Saravanamurugan, B. Song, S. Yang, *ACS Catal.*, 6 (2016) 7722-7727.
- [43] T. Wang, A. Hu, G. Xu, C. Liu, H. Wang, Y. Xia, *Catal. Lett.*, 149 (2019) 1845-1855.
- [44] F. Li, L.J. France, Z. Cai, Y. Li, S. Liu, H. Lou, J. Long, X. Li, *Appl. Catal. B-Environ.*, 214 (2017) 67-77.

Journal Pre-proof